

Sivers and Boer-Mulders distributions in boost-invariant longitudinal position space

Tanmay Maji^{1,*}

¹*Department of Physics, National Institute of Technology Kurukshetra, India 136119*

(Dated: August 8, 2024)

The boost invariant longitudinal position space variable σ , the Fourier conjugate to skewness ξ , unravels the longitudinal impact parameter information in a proton. Here, we investigate skewness sensitivity of T-odd leading twist GTMDs considering a momentum transfer to longitudinal as well as in transverse direction and present a detailed study of the spin-transverse momentum correlation through Sivers and Boer-Mulders Wigner Distributions in boost invariant longitudinal position space. The σ -space distributions of T-odd sector shows oscillatory patterns sensitive to square of the total momentum transfer $-t$, analogous to the diffraction scattering of wave in Optics. An additional effect on the diffraction pattern is reported caused by interference between transverse momentum transfer Δ_{\perp} to the transverse momentum \mathbf{p}_{\perp} of quarks.

I. INTRODUCTION

This quest to understand the internal structure of hadrons involves unravelling the partonic distributions of quarks and gluons and their correlations within the hadron. The recent time advanced theoretical frameworks that significantly contribute to understanding of three dimensional tomography of proton are the Generalized Transverse Momentum Distributions (GTMDs) and Wigner distribution(WDs). Under certain limit, GTMDs reduces to Generalized Parton Distributions (GPDs) and Transverse Momentum Distributions (TMDs) which have been fundamental in advancing our understanding of the three-dimensional partonic structure of protons. The GPDs appear in hard exclusive reactions like deeply virtual Compton scattering (DVCS) or deeply virtual meson production (DVMP), whereas the TMDs are accessible in the description of semi-inclusive reactions like semi-inclusive deep inelastic scattering (SIDIS) and Drell-Yan process [1–5].

However, a more comprehensive framework that integrates the features of both GPDs and TMDs is provided by Generalized Transverse Momentum Distributions (GTMDs) which encapsulate a richer set of information incorporating both the transverse momentum and spatial distributions of parton. One of the intriguing aspects of GTMDs is their sensitivity to the skewness parameter, which represents the longitudinal momentum transfer between the initial and final states of the proton. While, $\xi = 0$ indicates that the momentum transfer occurs solely in the transverse direction. Most prior analyses of nucleon GTMDs have assumed momentum transfer only in the transverse direction. However, experimental observations consistently involve $\xi \neq 0$. Therefore, it is important to develop a more comprehensive understanding of GTMDs at non-zero skewness. The GTMDs with non-zero skewness offer insights into the off-forward kinematics of parton distributions and provide a window into more complete three-dimensional tomography of the proton, e.g., deeply virtual Compton scattering (DVCS) and hard exclusive meson production (DVMP) [6–9], where the skewness parameter ξ plays a significant role. GTMDs with non-zero skewness adds a new dimension to the study of proton structure, that are not accessible through GPDs and TMDs alone.

Particularly the Time-reversal odd (T-odd) GTMDs are crucial as they are sensitive to the complex spin and momentum correlations within the proton. The T-odd GTMDs provide insights into phenomena such as Single-Spin Asymmetries (SSA)[10, 11] and the underlying mechanisms of parton orbital angular momentum. Under the bilinear decomposition of the GTMDs correlator, all the polarization specific GTMDs, in principle, can have T-odd part along with T-even part and be expressed as $\chi_{i,j} = \chi_{i,j}^{(e)} + i\chi_{i,j}^{(o)}$. Most of the T-odd parts missing its physical significant so far, however, few of them show important roll in physical phenomenon e.g., Sivers and Boer-Mulders asymmetry, spin density of quarks etc. We consider semi-inclusive deep inelastic scattering process (SIDIS) and focus on such T-odd distributions $F_{1,2}^{(o)}$ and $H_{1,1}^{(o)}$ with non-zero skewness associated with Sivers and Boer-Mulders asymmetries. The quark GTMDs can be accessed through the physical exclusive double Drell–Yan process [12], while the gluon GTMDs are measurable in diffractive di-jet production in deep-inelastic lepton-nucleon and lepton-nucleus scattering [13–16] and ultra-peripheral proton-nucleus collisions [17], as well as in virtual photon-nucleus quasi-elastic scattering [18].

The Wigner distribution, a quasi-probability distribution in phase space, provides a comprehensive picture of the partonic structure of the proton by incorporating both spatial and momentum distributions. Wigner distribution in

*Electronic address: tanmayphy@nitkkr.ac.in

impact parameter space \mathbf{b}_\perp is obtained by taking the Fourier transform of GTMDs with respect to the transverse momentum transfer Δ_\perp , more precisely, \mathbf{b}_\perp is Fourier conjugate to $\mathbf{D}_\perp = \frac{\mathbf{b}_\perp}{(1-\xi^2)}$ for the case of non-zero skewness ξ [19–22]. It allows investigation of various partonic correlations, including spin-spin and spin-orbit interactions, and their dependence on the transverse position within the proton [23]. In the context of Quantum Chromodynamics (QCD), the Wigner distributions were introduced in Ji [24] and have been extensively explored the transverse impact parameter space configuration of hadrons [23, 25–41]. Recent advancements in the study of Wigner distributions, particularly in the boost-invariant longitudinal space of the proton, have garnered significant attention due to their potential to offer deeper insights into hadronic structure. A key development in this area involves the exploration of Wigner distributions in the boost-invariant longitudinal position space, denoted as σ . This coordinate is defined as $\sigma = \frac{1}{2}b^-P^+$, where b^- is the longitudinal impact parameter and P^+ is the longitudinal momentum of the proton. The Fourier transform of GTMDs with respect to the skewness variable ξ yields the Wigner distributions in the longitudinal position space σ . In light-front models framework, the σ -space have been investigated for other primary distributions e.g., the DVCS amplitudes and the GPDs of a relativistic spin- $\frac{1}{2}$ composite system [42–45] in various models including those inspired by AdS/QCD [46, 47] and phenomenological GPD models [43–45, 48–51]. A notable features observed in longitudinal position space distribution is a diffraction pattern analogous to the diffractive scattering of a wave in optics. Additionally, the Wigner distributions in the boost-invariant longitudinal space have been shown to exhibit long-distance tails [52].

Recently, we have presented T-even GTMDs and quark Wigner distribution in boost invariant longitudinal position space for proton in the LFQDM [46] and observed diffractive phenomenon analogous to wave optics. This motivates the investigation of the T-odd sector of the leading twist-Wigner distributions of proton in boost invariant longitudinal position space which encodes information of spin-orbit interactions that led to the Sivers and Boer-Mulders Asymmetry.

This paper aims to explore leading-twist T-odd GTMDs of proton with non-zero skewness using the extended light-front quark diquark model framework within the Dokshitzer Gribov Lipatov Altarelli Parisi (DGLAP) region. In this model the T-odd sector is determined incorporating the contribution from final state interaction (FSI) and the wave function of the model is constructed in the framework of AdS/QCD soft-wall model. A brief overview of the T-odd sector in the Light-Front Quark Diquark Model (LFQDM) is given in the Sec.II. The kinematics and definition of T-odd GTMD with skewness is included in Sec.III which contains analytical and numerical results of T-odd GTMDs in this model. In Sec.III B, the model results for quark spin density is presented. In Sec.IV, we present the results and discussions on boost invariant longitudinal space for the Sivers and Boer-Mulders distributions. For completeness, the model results for Sivers and Boer-Mulder distributions in transverse impact parameter space are presented in Sec.V.

II. T-ODD SECTOR IN LIGHT-FRONT QUARK-DIQUARK MODEL

The Light-Front Quark Diquark Model (LFQDM) is a theoretical framework simplifies the complex interactions of quarks and gluons by treating proton as a bound state of a quark and a diquark [53]. In this model, both scalar and axial vector diquarks are considered, and the light-front wave functions (LFWFs) are derived from the two-particle effective wave functions obtained in the soft-wall AdS/QCD framework. It has been successfully used to describe various interesting properties of the nucleon, such as axial charge, tensor charge, PDFs, GPDs, TMDs, Wigner distributions at zero skewness, and spin asymmetries [23, 53–59]. Recently, the T-even GTMDs at non-zero skewness for all polarization of proton are presented in [46].

In LFQDM, considering $SU(4)$ spin-flavor symmetry, the proton state $|P; \pm\rangle$ is written as superposition of the quark-diquark states as $|P; \pm\rangle = C_S|u S^0\rangle^\pm + C_V|u A^0\rangle^\pm + C_{VV}|d A^1\rangle^\pm$ where C_S, C_V and C_{VV} are the coefficients of isoscalar-scalar diquark singlet state $|u S^0\rangle$, isoscalar-vector diquark state $|u A^0\rangle$ and isovector-vector diquark state $|d A^1\rangle$ respectively [53, 60, 61].

For scalar diquark, the two-particle Fock-state expansion with $J^z = \pm 1/2$ is given by

$$|u S\rangle^\pm = \int \frac{dx d^2\mathbf{p}_\perp}{2(2\pi)^3\sqrt{x(1-x)}} \sum_{\lambda_q=\pm 1/2} \psi_{\lambda_q}^{\pm(u)}(x, \mathbf{p}_\perp) |\lambda_q s; xP^+, \mathbf{p}_\perp\rangle, \quad (1)$$

where $|\lambda_q s; xP^+, \mathbf{p}_\perp\rangle$ represents two-particle singlet state with scalar diquark of helicity $\lambda_S = 0$. The light-front wave functions (LFWFs), with nucleon helicities $\lambda_N = \pm$ and for quark $\lambda_q = \pm$, denoted by $\psi_{\lambda_q}^{\lambda_N(u)}(x, \mathbf{p}_\perp)$ have

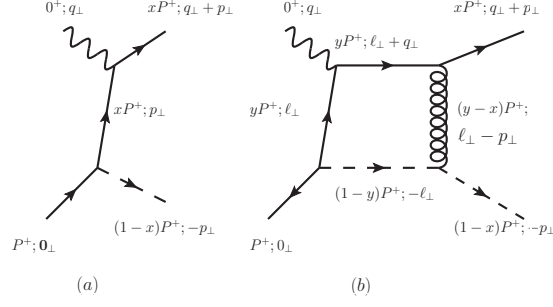


FIG. 1: SIDIS process at (a) tree level and (b) including final-state interaction (FSI)

explicit form for different combination of spin (plus and minus correspond to $+\frac{1}{2}$ and $-\frac{1}{2}$, respectively) as [58, 62, 63]

$$\begin{aligned}
 \psi_+^{+(u)}(x, \mathbf{p}_\perp) &= \psi_-^{-(u)}(x, \mathbf{p}_\perp) = N_S \left[1 + i \frac{e_1 e_2}{8\pi} (\mathbf{p}_\perp^2 + B) g_1 \right] \varphi_1^{(u)}(x, \mathbf{p}_\perp), \\
 \psi_-^{+(u)}(x, \mathbf{p}_\perp) &= N_S \left(-\frac{p^1 + ip^2}{xM} \right) \left[1 + i \frac{e_1 e_2}{8\pi} (\mathbf{p}_\perp^2 + B) g_2 \right] \varphi_2^{(u)}(x, \mathbf{p}_\perp), \\
 \psi_+^{-(u)}(x, \mathbf{p}_\perp) &= N_S \left(\frac{p^1 - ip^2}{xM} \right) \left[1 + i \frac{e_1 e_2}{8\pi} (\mathbf{p}_\perp^2 + B) g_2 \right] \varphi_2^{(u)}(x, \mathbf{p}_\perp),
 \end{aligned} \tag{2}$$

Meanwhile, the state with spin-1 diquark is expressed as

$$|\nu A\rangle^\pm = \int \frac{dx d^2 \mathbf{p}_\perp}{2(2\pi)^3 \sqrt{x(1-x)}} \sum_{\lambda_q = \pm 1/2} \sum_{\lambda_D = \pm 1, 0} \psi_{\lambda_q \lambda_D}^{\pm(\nu)}(x, \mathbf{p}_\perp) |\lambda_q \lambda_D; xP^+, \mathbf{p}_\perp\rangle, \tag{3}$$

where $|\lambda_q \lambda_D; xP^+, \mathbf{p}_\perp\rangle$ is corresponding to the two-particle state with the axial-vector diquark of helicities $\lambda_D = \pm 1, 0$ (triplet). While, the wavefunctions $\psi_{\lambda_q, \lambda_D}^{\lambda_N(u)}(x, \mathbf{p}_\perp)$ for axial-vector diquark (for $J = \pm 1/2$) carries an additional subscript corresponding to the non-singlet diquark helicities and the explicit form for different combination is given by [58]

$$\begin{aligned}
 \psi_{++}^{+(\nu)}(x, \mathbf{p}_\perp) &= \frac{(p^1 - ip^2)^2}{\mathbf{p}_\perp^2} \psi_{--}^{-(\nu)}(x, \mathbf{p}_\perp) = N_1^{(\nu)} \sqrt{\frac{2}{3}} \left(\frac{p^1 - ip^2}{xM} \right) \left[1 + i \frac{e_1 e_2}{8\pi} (\mathbf{p}_\perp^2 + B) g_2 \right] \varphi_2^{(\nu)}(x, \mathbf{p}_\perp), \\
 \psi_{-+}^{+(\nu)}(x, \mathbf{p}_\perp) &= -\psi_{+-}^{-(\nu)}(x, \mathbf{p}_\perp) = N_1^{(\nu)} \sqrt{\frac{2}{3}} \left[1 + i \frac{e_1 e_2}{8\pi} (\mathbf{p}_\perp^2 + B) g_1 \right] \varphi_1^{(\nu)}(x, \mathbf{p}_\perp), \\
 \psi_{+0}^{+(\nu)}(x, \mathbf{p}_\perp) &= -\psi_{-0}^{-(\nu)}(x, \mathbf{p}_\perp) = -N_0^{(\nu)} \sqrt{\frac{1}{3}} \left[1 + i \frac{e_1 e_2}{8\pi} (\mathbf{p}_\perp^2 + B) g_1 \right] \varphi_1^{(\nu)}(x, \mathbf{p}_\perp), \\
 \psi_{-0}^{+(\nu)}(x, \mathbf{p}_\perp) &= \frac{(p^1 + ip^2)^2}{\mathbf{p}_\perp^2} \psi_{+0}^{-(\nu)}(x, \mathbf{p}_\perp) = N_0^{(\nu)} \sqrt{\frac{1}{3}} \left(\frac{p^1 + ip^2}{xM} \right) \left[1 + i \frac{e_1 e_2}{8\pi} (\mathbf{p}_\perp^2 + B) g_2 \right] \varphi_2^{(\nu)}(x, \mathbf{p}_\perp),
 \end{aligned} \tag{4}$$

$$\psi_{+-}^{+(\nu)}(x, \mathbf{p}_\perp) = \psi_{--}^{+(\nu)}(x, \mathbf{p}_\perp) = \psi_{++}^{-(\nu)}(x, \mathbf{p}_\perp) = \psi_{-+}^{-(\nu)}(x, \mathbf{p}_\perp) = 0,$$

with normalization constants $N_S, N_0^{(\nu)}$ and $N_1^{(\nu)}$ for the respective flavour $\nu = u, d$. The wave functions are normalized according to the quark counting rules [53]. The imaginary part of the wave functions are consistent with the final state interaction (FSI) amplitude [4]. In the imaginary part, term g_1, g_2 are given by

$$g_1 = \int_0^1 d\alpha \frac{-1}{\alpha(1-\alpha)\mathbf{p}_\perp^2 + \alpha m_g^2 + (1-\alpha)B}, \tag{5}$$

$$g_2 = \int_0^1 d\alpha \frac{-\alpha}{\alpha(1-\alpha)\mathbf{p}_\perp^2 + \alpha m_g^2 + (1-\alpha)B}, \tag{6}$$

and \mathbf{p}_\perp independent term B has explicit form

$$B = x(1-x)(-M^2 + \frac{m_q^2}{x} + \frac{m_D^2}{1-x}), \quad (7)$$

with proton mass M , struck quark and diquark mass m_q and m_D , and gluon mass m_g . The gluon mass is taken as zero at the end of the calculations. Here, the final state interaction is governed by a gluon and e_1, e_2 are the color charge of the struck quark and diquark, respectively. Thus, FSI gauge exchange strength is considered as $\frac{e_1 e_2}{4\pi} \rightarrow -C_F \alpha_s$ with color factor C_F . The LFWFs $\varphi_i^{(\nu)}(x, \mathbf{p}_\perp)$ are the modified form of the soft-wall AdS/QCD prediction and the two particle effective wave functions reads as

$$\varphi_i^{(\nu)}(x, \mathbf{p}_\perp) = \frac{4\pi}{\kappa} \sqrt{\frac{\log(1/x)}{1-x}} x^{a_i^\nu} (1-x)^{b_i^\nu} \exp \left[-\frac{\mathbf{p}_\perp^2 \log(1/x)}{2\kappa^2 (1-x)^2} \right], \quad (8)$$

with flavour index $\nu = u, d$. The modification is incorporated through the parameters a_i^ν, b_i^ν and φ_i^ν ($i = 1, 2$) of Eq.8 reduce to the original AdS/QCD wave function [64, 65] at the limit $a_i^\nu = b_i^\nu = 0$. We use the AdS/QCD scale parameter $\kappa = 0.4$ GeV [66, 67] and the quarks are assumed to be massless. The parameters of this model are obtained by fitting the flavor-decomposed Dirac and Pauli form factors data, as detailed in Refs. [53, 55]. The wave functions generated by this model, using these parameters, show a reasonably good agreement with the proton electric and magnetic charge radius data, axial charge and tensor charge as well as parton distribution measurements.

III. T-ODD GTMDS WITH NON-ZERO SKEWNESS

In deep inelastic scattering, a proton of average momentum P interacts with lepton via a photon of virtuality $Q^2 = -q^2$. Eventually, the high energy virtual photon interacts with the interior parton of momentum p which carries longitudinal momentum fraction $x = p^+/P^+$ and transverse momentum \mathbf{p}_\perp . The momentum transfer to the system is defined by Δ and $-t = \Delta^2$. For such interaction, the GTMDs correlator is defined at the fixed light cone time $z^+ = 0$ as [68, 69]

$$W_{[\lambda''\lambda']}^{\nu[\Gamma]}(x, \xi, \Delta_\perp^2, \mathbf{p}_\perp^2, \mathbf{p}_\perp \cdot \Delta_\perp) = \frac{1}{2} \int \frac{dz^-}{(2\pi)} \frac{d^2 z_T}{(2\pi)^2} e^{ip \cdot z} \langle P''; \lambda'' | \bar{\psi}^\nu(-z/2) \Gamma \mathcal{W}_{[-z/2, z/2]} \psi^\nu(z/2) | P'; \lambda' \rangle \Big|_{z^+=0}, \quad (9)$$

where $|P'; \lambda'\rangle$ and $|P''; \lambda''\rangle$ are the initial and final states of the proton with helicities λ' and λ'' , respectively. The bi-local operator with quark fields ψ and $\bar{\psi}$ are at two different points linked by the gauge link gauge $\mathcal{W}_{[-z/2, z/2]}$ which is chosen to be unity[Ref]. Dirac γ -matrices, i.e., $\Gamma = \{\gamma^+, \gamma^+ \gamma^5, i\sigma^{j+} \gamma^5\}$ are chosen to extract the contribution of unpolarized, longitudinally polarized and transversely polarized quarks, respectively. In the symmetric frame, the average four-momentum of proton $P = \frac{1}{2}(P'' + P')$ can be written as

$$P \equiv \left(P^+, \frac{M^2 + \Delta_\perp^2/4}{(1 - \xi^2)P^+}, \mathbf{0}_\perp \right), \quad (10)$$

where, the initial (P') and final (P'') momentum of proton are given by

$$P' \equiv \left((1 + \xi)P^+, \frac{M^2 + \Delta_\perp^2/4}{(1 + \xi)P^+}, -\Delta_\perp/2 \right), \quad (11)$$

$$P'' \equiv \left((1 - \xi)P^+, \frac{M^2 + \Delta_\perp^2/4}{(1 - \xi)P^+}, \Delta_\perp/2 \right). \quad (12)$$

The interior parton has non-zero transverse momentum $p \equiv (xP^+, p^-, \mathbf{p}_\perp)$, and sum of transverse momenta of all the constituent partons vanishes which satisfies the zero transverse momentum of the proton *e.g.*, $P_\perp = \sum_i \mathbf{p}_\perp^i = 0$. In a symmetric frame the energy transferred to the system $\Delta = (P'' - P')$ reads as

$$\Delta \equiv \left(-2\xi P^+, \frac{t + \Delta_\perp^2}{-2\xi P^+}, \Delta_\perp \right), \quad (13)$$

where, skewness is defined as $\xi = -\Delta^+/2P^+$. Energy transferred to the process is measured as square of total momentum transfer $t = \Delta^2$ and an explicit relation can be established using $\Delta^- = (P''^- - P'^-)$ as

$$-t = \frac{4\xi^2 M^2 + \Delta_\perp^2}{(1 - \xi^2)}. \quad (14)$$

Here, the definition of skewness ξ is adopted from convention in Ref. [69], which is differed by a minus sign with respect to the definition in Ref. [70].

For a spin-1/2 hadron, bilinear decomposition of the fully unintegrated quark-quark correlator is parameterized in terms of GTMDs as [69].

$$W_{[\lambda''\lambda']}^{\nu[\gamma^+]}(x, \xi, \Delta_\perp^2, \mathbf{p}_\perp^2, \mathbf{p}_\perp \cdot \Delta_\perp) = \frac{1}{2M} \bar{u}(P'', \lambda'') \left[\dots + \frac{i\sigma^{i+} p_\perp^i}{P^+} F_{1,2}(x, \xi, \Delta_\perp^2, \mathbf{p}_\perp^2, \mathbf{p}_\perp \cdot \Delta_\perp) + \dots \right] u(P', \lambda'), \quad (15)$$

$$W_{[\lambda''\lambda']}^{\nu[i\sigma^{j+}\gamma^5]}(x, \xi, \Delta_\perp^2, \mathbf{p}_\perp^2, \mathbf{p}_\perp \cdot \Delta_\perp) = \frac{1}{2M} \bar{u}(P'', \lambda'') \left[-\frac{i\epsilon_\perp^{ij} p_\perp^i}{M} H_{1,1}(x, \xi, \Delta_\perp^2, \mathbf{p}_\perp^2, \mathbf{p}_\perp \cdot \Delta_\perp) + \dots \right] u(P', \lambda'), \quad (16)$$

with the four component Dirac-spinor $u(k, \lambda)$ of momentum k and the helicity $\lambda (= \pm)$. The explicit form of the Dirac spinors are appended in App.A. We concentrate on the unpolarised and transversely polarised partons and corresponding Dirac structures $\Gamma = \gamma^+, i\sigma^{j+}\gamma^5$ respectively as these two encode T-odd distributions related to Sivers and Boer-Mulders distributions. The dots in the right hand side of Eq.(15,16) indicate other leading twist GTMDs having different bilinear pre-factors whose complete discussion is given in [69]. All the GTMDs can be written in terms of time reversal even (T-even) and time reversal odd (T-odd) parts as

$$\mathcal{X}_{i,j}(x, \xi, \Delta_\perp^2, \mathbf{p}_\perp^2, \mathbf{p}_\perp \cdot \Delta_\perp) = \mathcal{X}_{i,j}^e(x, \xi, \Delta_\perp^2, \mathbf{p}_\perp^2, \mathbf{p}_\perp \cdot \Delta_\perp) + i\mathcal{X}_{i,j}^o(x, \xi, \Delta_\perp^2, \mathbf{p}_\perp^2, \mathbf{p}_\perp \cdot \Delta_\perp) \quad (17)$$

where \mathcal{X} stands for any GTMDs at leading twist. Using the two-particle Fock-state expansion of Eqs.(1,3) in the Eq.(9), the GTMDs correlators can be expressed in terms of overlap representation as

$$\begin{aligned} W_{[\lambda''\lambda']}^{\nu[\gamma^+]}(x, \xi, \Delta_\perp^2, \mathbf{p}_\perp^2, \mathbf{p}_\perp \cdot \Delta_\perp) &= C_S^2 \frac{1}{16\pi^3} \sum_{\lambda_q} \psi_{\lambda_q}^{\lambda''\dagger}(x'', \mathbf{p}_\perp'') \psi_{\lambda_q}^{\lambda'\dagger}(x', \mathbf{p}_\perp') \\ &\quad + C_A^2 \frac{1}{16\pi^3} \sum_{\lambda_q} \sum_{\lambda_D} \psi_{\lambda_q \lambda_D}^{\lambda''\dagger}(x'', \mathbf{p}_\perp'') \psi_{\lambda_q \lambda_D}^{\lambda'\dagger}(x', \mathbf{p}_\perp') \end{aligned} \quad (18)$$

$$\begin{aligned} W_{[\lambda''\lambda']}^{\nu[i\sigma^{j+}\gamma^5]}(x, \xi, \Delta_\perp^2, \mathbf{p}_\perp^2, \mathbf{p}_\perp \cdot \Delta_\perp) &= C_S^2 \frac{1}{16\pi^3} \sum_{\lambda_q'} \sum_{\lambda_q} (2\lambda_q' i)^i \psi_{\lambda_q'}^{\lambda''\dagger}(x'', \mathbf{p}_\perp'') \psi_{\lambda_q}^{\lambda'\dagger}(x', \mathbf{p}_\perp') \\ &\quad + C_A^2 \frac{1}{16\pi^3} \sum_{\lambda_q'} \sum_{\lambda_q} \sum_{\lambda_D} \epsilon_\perp^{ij} (2\lambda_q' i)^i \psi_{\lambda_q' \lambda_D}^{\lambda''\dagger}(x'', \mathbf{p}_\perp'') \psi_{\lambda_q \lambda_D}^{\lambda'\dagger}(x', \mathbf{p}_\perp') \end{aligned} \quad (19)$$

where, $C_A = C_V, C_{VV}$ for u and d quarks respectively [53]. The explicit form of the initial and final transverse momenta of the struck quark are given by

$$\mathbf{p}_\perp' = \mathbf{p}_\perp - (1 - x') \frac{\Delta_\perp}{2}, \quad \text{with } x' = \frac{x + \xi}{1 + \xi}, \quad (20)$$

$$\mathbf{p}_\perp'' = \mathbf{p}_\perp + (1 - x'') \frac{\Delta_\perp}{2}, \quad \text{with } x'' = \frac{x - \xi}{1 - \xi}, \quad (21)$$

respectively.

A. Model Results for GTMDs

In this LFQDM, the GTMD-correlator is written in terms of the scalar and the axial-vector diquark components as

$$W_{[\lambda''\lambda']}^{\nu[\Gamma]}(x, \mathbf{p}_\perp, \Delta_\perp) = C_S^2 W_{[\lambda''\lambda']}^{\nu[\Gamma](S)}(x, \mathbf{p}_\perp, \Delta_\perp) + C_A^2 W_{[\lambda''\lambda']}^{\nu[\Gamma](A)}(x, \mathbf{p}_\perp, \Delta_\perp), \quad (22)$$

where, $C_A = C_V, C_{VV}$ for u and d quarks respectively.

In this work, our main concern is to address $F_{1,2}^o(x, \xi, \Delta_\perp^2, \mathbf{p}_\perp^2, \mathbf{p}_\perp \cdot \Delta_\perp)$ and $H_{1,1}^o(x, \xi, \Delta_\perp^2, \mathbf{p}_\perp^2, \mathbf{p}_\perp \cdot \Delta_\perp)$ which reduced to the Sivers and Boer-Mulders functions respectively at the TMDs limit $\xi = 0, \Delta_\perp = 0$. From the overlap representation of Eq.(18,19) and the bilinear decomposition of Eq.(15,16), the final results of odd part of the GTMDs

in this model reads as

$$F_{1,2}^{(o)\nu}(x, \xi, \Delta_{\perp}^2, \mathbf{p}_{\perp}^2, \Delta_{\perp} \cdot \mathbf{p}_{\perp}) = \frac{1}{16\pi^3} \left[N_{F12}^{\nu} \frac{1}{\sqrt{1-\xi^2}} \left\{ (\chi_1'' - \chi_2') \frac{A_1^{\nu}(x'') A_2^{\nu}(x')}{x'} - (\chi_2'' - \chi_1') \frac{A_2^{\nu}(x'') A_1^{\nu}(x')}{x''} \right\} \right. \\ \left. - \frac{\Delta_{\perp}^2}{2M^2} N_{F14}^{\nu} \frac{\xi}{(1-\xi^2)^{3/2}} \frac{(1-x)}{x'' x'} (\chi_2'' - \chi_2') A_2^{\nu}(x'') A_2^{\nu}(x') \right] \exp \left[-\tilde{a}(x'') \mathbf{p}_{\perp}^{\prime 2} - \tilde{a}(x') \mathbf{p}_{\perp}^{\prime 2} \right], \quad (23)$$

$$H_{1,1}^{(o)\nu}(x, \xi, \Delta_{\perp}^2, \mathbf{p}_{\perp}^2, \Delta_{\perp} \cdot \mathbf{p}_{\perp}) = N_{H11}^{\nu} \frac{1}{16\pi^3} \sqrt{1-\xi^2} \left[(\chi_1'' - \chi_2') \frac{A_1^{\nu}(x'') A_2^{\nu}(x')}{x'} - (\chi_2'' - \chi_1') \frac{A_2^{\nu}(x'') A_1^{\nu}(x')}{x''} \right] \\ \times \exp \left[-\tilde{a}(x'') \mathbf{p}_{\perp}^{\prime 2} - \tilde{a}(x') \mathbf{p}_{\perp}^{\prime 2} \right], \quad (24)$$

Where,

$$A_i^{\nu}(x) = \frac{4\pi}{\kappa} \sqrt{\frac{\log(1/x)}{1-x}} x^{a_i^{\nu}} (1-x)^{b_i^{\nu}}, \quad (25)$$

$$\tilde{a}(x) = \frac{\log(1/x)}{2\kappa^2(1-x)^2}; \quad \text{and} \quad a(x) = 2\tilde{a}(x). \quad (26)$$

The contribution from imaginary part of the wave function is denoted by

$$(\chi_1'' - \chi_2') = \frac{1}{2} C_F \alpha_S \left[\ln \left(1 + \frac{\mathbf{p}_{\perp}^{\prime 2}}{B(x'')} \right) + \frac{B(x')}{\mathbf{p}_{\perp}^{\prime 2}} \ln \left(1 + \frac{\mathbf{p}_{\perp}^{\prime 2}}{B(x')} \right) \right], \quad (27)$$

$$(\chi_2'' - \chi_1') = -\frac{1}{2} C_F \alpha_S \left[\frac{B(x'')}{\mathbf{p}_{\perp}^{\prime 2}} \ln \left(1 + \frac{\mathbf{p}_{\perp}^{\prime 2}}{B(x'')} \right) + \ln \left(1 + \frac{\mathbf{p}_{\perp}^{\prime 2}}{B(x')} \right) \right], \quad (28)$$

$$(\chi_2'' - \chi_2') = -\frac{1}{2} C_F \alpha_S \left[\frac{B(x'')}{\mathbf{p}_{\perp}^{\prime 2}} \ln \left(1 + \frac{\mathbf{p}_{\perp}^{\prime 2}}{B(x'')} \right) - \frac{B(x')}{\mathbf{p}_{\perp}^{\prime 2}} \ln \left(1 + \frac{\mathbf{p}_{\perp}^{\prime 2}}{B(x')} \right) \right]. \quad (29)$$

These combinations cancel out the divergent part of the integration function g_1 and g_2 and produced finite contribution. At $\xi = 0$ limit, difference in longitudinal fractions of incoming and outgoing partons vanishes $x' = x'' = x$ and the exponential term becomes independent of $\mathbf{p}_{\perp} \cdot \Delta_{\perp}$. The third term of Eq.23 vanishes at the zero-skewness. The normalization constants of the distributions are denoted by $N_{F12}^{\nu} = (C_S^2 N_S^2 - C_A^2 \frac{1}{3} N_0^2)^{\nu}$, $N_{F14}^{\nu} = (C_S^2 N_S^2 + C_A^2 (\frac{1}{3} N_0^2 - \frac{2}{3} N_1^2))^{\nu}$, $N_{H11}^{\nu} = (C_S^2 N_S^2 + C_A^2 (\frac{1}{3} N_0^2 + \frac{2}{3} N_1^2))^{\nu}$. For completeness, the LFQDM results for all the other leading twist T-odd GTMDs are listed up in App.A.

Here we present model results of the T-odd GTMDs numerically and concentrate on the skewness variation. The model parameters are taken from Ref. with proton mass $M = 0.94 \text{ GeV}$, diquark mass $m_D = 0.98 \pm 0.04 \text{ GeV}$. In principle the mass of diquark has lower bound given by the proton mass to satisfy the condition of stable bound state proton. However, the upper bound of m_D is restrict by the spin sum rule [71]. The quarks are considered to be massless.

Fig.2 represents the illustration of flavor dependent T-odd GTMDs $F_{1,2}^{(0)}$ and $H_{1,1}^{(0)}$ in three-dimension of longitudinal momentum fraction x and skewness ξ . We consider the DGLAP region where the longitudinal momentum fraction is restricted in between skewness ξ and its upper bound 1 i.e., $\xi < x < 1$. The upper row is for $F_{1,2}^{(0)}$ and the lower row is for $H_{1,1}^{(0)}$ distributions, while the left column shows for u -quark and right row is for d -quark. All these numerical results are computed for $\mathbf{p}_{\perp}^2 = 0.3 \text{ GeV}^2$ and $\Delta_{\perp}^2 = 0.2 \text{ GeV}^2$. We also consider the case when Δ_{\perp} is perpendicular to \mathbf{p}_{\perp} i.e., $\mathbf{p}_{\perp} \cdot \Delta_{\perp} = 0$. The GTMD, $F_{1,2}^{(0)}$, is the distribution associated to an unpolarised parton in a transversely polarised proton. The model result of $F_{1,2}^{(0)}$ in the DGLAP region shows a positive peak for u -quark and negative peak for d -quark and the peak belongs to the lower value of $x < 0.5$. The flip of polarity in $F_{1,2}^{(0)}$ with the change of flavor from u to d quark is the consequence of Spin and transverse momentum correlation that led to the Sivers Effect at TMD limits. Interestingly, the similar left-right shifting is noticed for the more generic GTMDs distributions. However, the magnitude of the shift varies with skewness ξ . More precisely, for u quark, the peak of the distribution shifts towards right as the momentum transfer in the longitudinal direction increases, while their magnitudes decrease. A similar right shift of peak is noticed for d -quarks with opposite polarity peak. The GTMD $H_{1,1}^{(0)}$ provides a distribution of transversely polarised quark in an unpolarized proton. The distributions $H_{1,1}^{(0)}$ in ξ - x plain show positive peaks for both u and d quarks. The peaks shifted towards right upto $x < 0.5$ and magnitude die out with the increase of ξ . While the intensity of the peak is higher for u -quark than the d -quark.

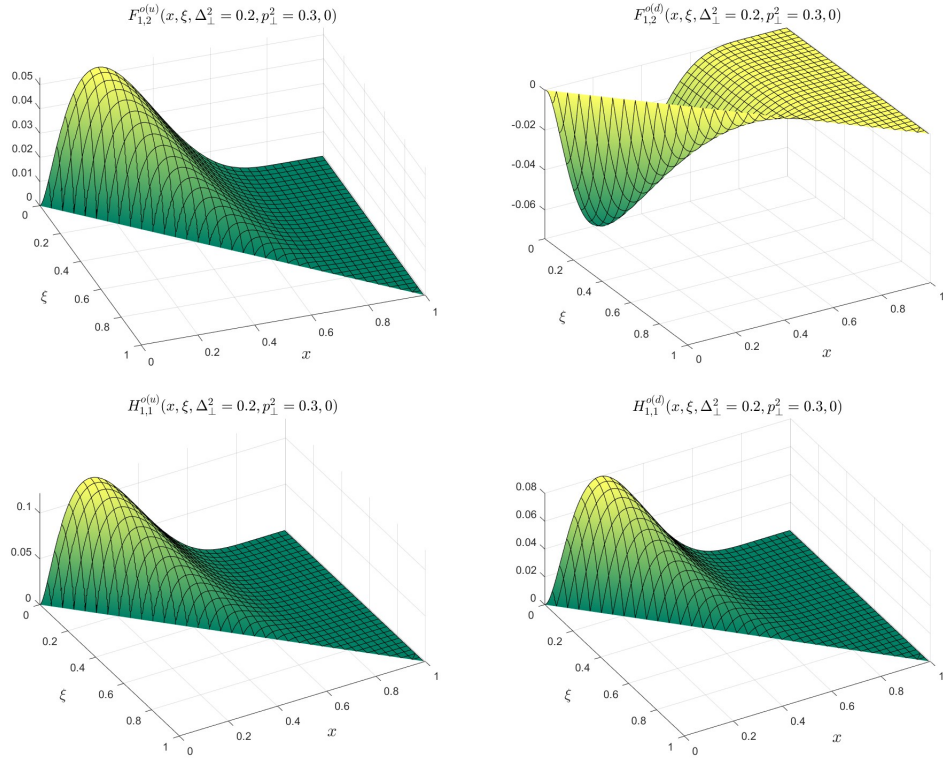


FIG. 2: Model results of $F_{1,2}^{(0)}$ (upper row) and $H_{1,1}^{(0)}$ (lower row) are shown in ξ - x plane for the DGLAP region $\xi < x < 1$. The left and right columns are for u and d quarks respectively with $\mathbf{p}_\perp^2 = 0.3 \text{ GeV}^2$ and $\Delta_\perp^2 = 0.2 \text{ GeV}^2$.

Fig.3 describes the x and Δ_\perp^2 dependence of Sivers (upper row) and Boer-Mulders (lower row) GTMDs at fixed $\xi = 0.1$ and $\mathbf{p}_\perp^2 = 0.2 \text{ GeV}^2$. Thus, in the DGLAP region, accessible space of x is $0.1 < x < 1$. The left and right columns are for u and d quarks respectively. The flavour decomposed results for Sivers and Boer-Mulders GTMDs, in x and Δ_\perp^2 , show almost similar general feature—the peaks of the distribution move towards larger values of x with increasing momentum transfer Δ_\perp^2 and the magnitudes of all the distributions decrease along x . To preserve the limited kinetic energy, the distributions in the transverse momentum broadens at higher- x which reflects a trend to carry a larger portion of the kinetic energy. Such general features are shown nearly model-independent properties for the GPDs and observed in several theoretical studies of the GPDs [49–51, 67, 72–79]. In this model, $F_{1,2}$ distribution flips polarity from positive to negative for u and d respectively. While, $H_{1,1}$ distributions remains positive irrespective of quark flavours. The different polarities of $F_{1,2}$ for the u and d quarks lead to the Sivers effect [10], which indicates an unpolarised quark distribution in a transversely polarized target has the transverse momentum asymmetry in perpendicular direction to proton spin.

B. Spin Density

The spin density of an unpolarised quark of skewness ξ in a transversely polarised proton can be defined in terms of GTMDs at vanishing transverse momentum transfer limit $\Delta_\perp = 0$ as

$$f_{\nu/P^\dagger}(x, \xi, \mathbf{p}_\perp) = \frac{1}{\sqrt{1-\xi^2}} F_{1,1}^e(x, \xi, 0, \mathbf{p}_\perp^2, 0) - \frac{\mathbf{S} \cdot (\hat{\mathbf{P}} \times \mathbf{p}_\perp)}{M} \sqrt{1-\xi^2} F_{1,2}^o(x, \xi, 0, \mathbf{p}_\perp^2, 0), \quad (30)$$

which satisfies the spin density defined in Ref.[80] at $\xi = 0$ limit. We are interested in effects of skewness ξ on the spin density. The model results for spin density is shown in Fig.(4), where the momentum of target proton \hat{P} is considered along the momentum transfer z -axis and proton spin S is taken along \hat{y} . As per the expectation, the model results are not symmetric and found left-shift for u and right shift for d quarks. Such left-right asymmetry can be explained from the numerical results, shown in Fig.2, for T-odd GTMDs $F_{1,2}^o$ of Eq.23. The mean-square transverse momentum

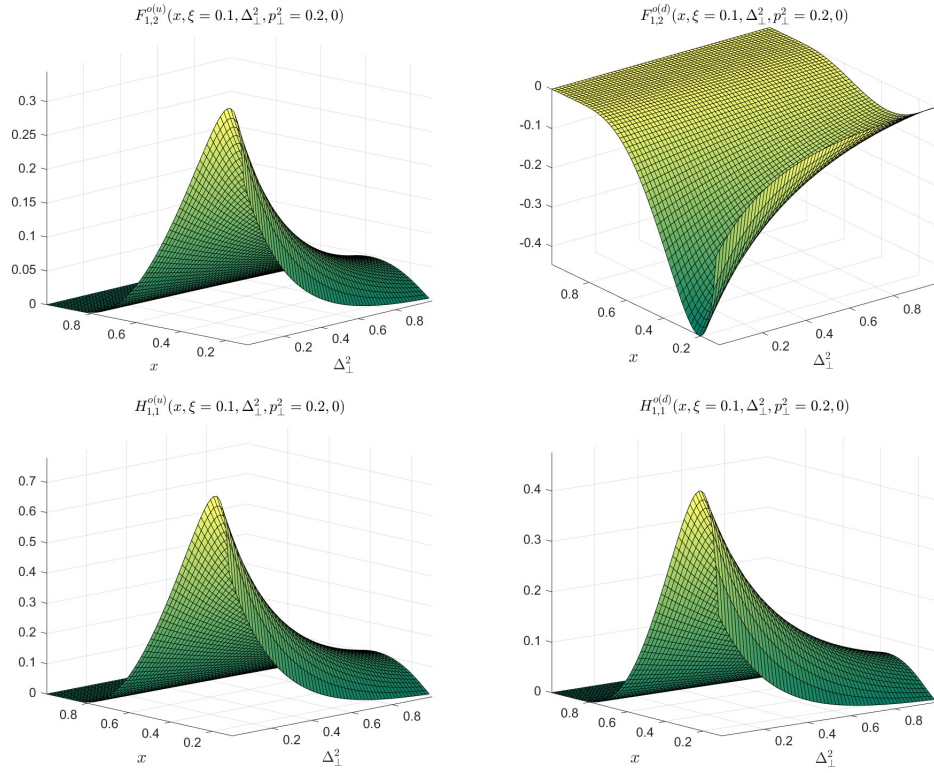


FIG. 3: Model results of $F_{1,2}^{(0)}$ (upper row) and $H_{1,1}^{(0)}$ (lower row) are shown in x - Δ_{\perp}^2 plane for the DGLAP region $\xi < x < 1$. The left and right columns are for u and d quarks respectively with $\xi = 0.1$ and $\mathbf{p}_{\perp}^2 = 0.2 \text{ GeV}^2$.

of the unpolarized quarks in a transversely polarised proton associated to spin density is given by

$$\langle \mathbf{p}_{\perp}^2 \rangle(\xi) = \int dx \int d^2 \mathbf{p}_{\perp} \mathbf{p}_{\perp}^2 f_{\nu/P^{\uparrow}}(x, \xi, \mathbf{p}_{\perp}) \quad (31)$$

which is sensitive to skewness variable ξ . In this model, $\langle \mathbf{p}_{\perp}^2 \rangle^u = \{0.131, 0.108, 0.081\}$ and $\langle \mathbf{p}_{\perp}^2 \rangle^d = \{0.075, 0.060, 0.042\}$ corresponding to the skewness $\xi = \{0, 0.1, 0.2\}$ respectively. Similarly, the model results for the spin density of transversely polarized quarks in an unpolarized proton shows an unidirectional left-shift for both u and d quarks as expected from the polarity non-flip distribution $H_{1,1}^{(0)}$, Fig.2.

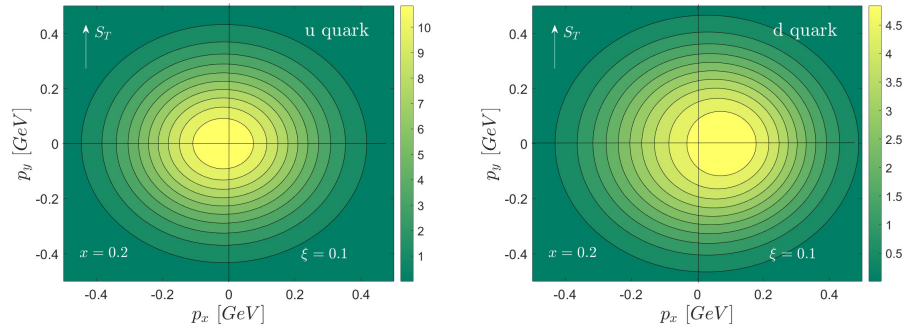


FIG. 4: Spin density for u -quark and d -quark in a transversely polarized proton with at $x = 0.2, \xi = 0.1$ and for the limit $\Delta_{\perp} = 0$. The transverse spin S_{\perp} is taken along \hat{y} .

IV. SIVERS AND BOER-MULDERS WDS IN BOOST INVARIANT LONGITUDINAL POSITION SPACE

In this section we discuss T-odd Wigner Distributions in boost-invariant longitudinal position space which is defined as a distribution in Fourier space to the skewness ξ . The Fourier conjugate to the skewness ξ is $\sigma = \frac{1}{2}b^-P^+$ and the WDs in boost invariant longitudinal position space is defined as

$$\tilde{\rho}^{\nu[\Gamma]}(x, \sigma, \Delta_{\perp}, \mathbf{p}_{\perp}; S) = \int_0^{\xi_s} \frac{d\xi}{2\pi} e^{i\sigma \cdot \xi} W^{\nu[\Gamma]}(x, \xi, \Delta_{\perp}^2, \mathbf{p}_{\perp}^2, \Delta_{\perp} \cdot \mathbf{p}_{\perp}; S), \quad (32)$$

where, the Wigner correlator $W^{\nu[\Gamma]}(x, \xi, \Delta_{\perp}^2, \mathbf{p}_{\perp}^2, \Delta_{\perp} \cdot \mathbf{p}_{\perp}; S)$ is given in Eq.(9) with $\lambda'' = \lambda' = S$. In this Fourier transformation, finiteness of the upper-limit ξ_s is restricted by the allowed range given by ξ_{max} as

$$\xi_{max} = \frac{(-t)}{2M^2} \left(\sqrt{1 + \frac{4M^2}{(-t)}} - 1 \right), \quad (33)$$

where M is the mass of target proton [43, 44, 70]. We restrict ourself to the DGLAP region $\xi < x < 1$ and the limit of the Fourier transform in σ -space is taken as $\xi_s = \xi_{max}$ if $\xi_{max} < x$ and $\xi_s = x$ for $\xi_{max} > x$, determined by a fixed value of $-t$. Following the similar prescription for polarization configurations of Wigner distributions in the \mathbf{b}_{\perp} space [23, 26, 31], the WDs in the longitudinal position space are defined as

$$\tilde{\rho}_{TU}^{i\nu}(x, \sigma, \Delta_{\perp}, \mathbf{p}_{\perp}) = \frac{1}{2} [\tilde{\rho}^{\nu[\gamma^+]}(x, \xi, \Delta_{\perp}^2, \mathbf{p}_{\perp}^2, \Delta_{\perp} \cdot \mathbf{p}_{\perp}; +\hat{S}_i) - \tilde{\rho}^{\nu[\gamma^+]}(x, \xi, \Delta_{\perp}^2, \mathbf{p}_{\perp}^2, \Delta_{\perp} \cdot \mathbf{p}_{\perp}; -\hat{S}_i)], \quad (34)$$

$$\tilde{\rho}_{UT}^{j\nu}(x, \sigma, \Delta_{\perp}, \mathbf{p}_{\perp}) = \frac{1}{2} [\tilde{\rho}^{\nu[i\sigma^{j+}\gamma^5]}(x, \xi, \Delta_{\perp}^2, \mathbf{p}_{\perp}^2, \Delta_{\perp} \cdot \mathbf{p}_{\perp}; +\hat{S}) - \tilde{\rho}^{\nu[i\sigma^{j+}\gamma^5]}(x, \xi, \Delta_{\perp}^2, \mathbf{p}_{\perp}^2, \Delta_{\perp} \cdot \mathbf{p}_{\perp}; -\hat{S})], \quad (35)$$

where, transverse index $i, j = \{1, 2\}$ for x and y direction respectively and the transverse spin of the proton is defined as $\hat{S}_j = \frac{1}{\sqrt{2}}(|+S\rangle + |-S\rangle)$. The subscripts of $\tilde{\rho}_{XY}^{j\nu}$ represent polarization of proton (by X) and of interior quark (by Y) respectively e.g., $\tilde{\rho}_{TU}^{j\nu}$ represents WDs of unpolarized quarks in a transversely polarised proton and $\tilde{\rho}_{UT}^{j\nu}$ is for the transversely polarised quark in unpolarised proton. For $\tilde{\rho}_{TU}^{j\nu}$, only the off-diagonal terms of Correlator $W_{[\lambda'' \lambda']}^{\nu[\Gamma]}$ contribute while for $\tilde{\rho}_{UT}^{j\nu}$ the diagonal terms contribute and can be written as

$$\begin{aligned} \hat{\rho}_{TU}^{i\nu}(x, \sigma, t, \mathbf{p}_{\perp}) &= -\frac{1}{2} \int_0^{\xi_s} \frac{d\xi}{2\pi} e^{i\sigma \cdot \xi} \epsilon_{\perp}^{ij}(i)^j \left[W_{[+-]}^{\nu[\gamma^+]}(x, \xi, \Delta_{\perp}^2, \mathbf{p}_{\perp}^2, \mathbf{p}_{\perp} \cdot \Delta_{\perp}) + (-1)^j W_{[-+]}^{\nu[\gamma^+]}(x, \xi, \Delta_{\perp}^2, \mathbf{p}_{\perp}^2, \mathbf{p}_{\perp} \cdot \Delta_{\perp}) \right] \\ &= \tilde{\rho}_{TU}^{i\nu}(x, \sigma, t, \mathbf{p}_{\perp}) + \frac{1}{M} \epsilon_{\perp}^{ij} p_{\perp}^j \tilde{\rho}_{Siv}^{\nu}(x, \sigma, t, \mathbf{p}_{\perp}), \end{aligned} \quad (36)$$

$$\begin{aligned} \hat{\rho}_{UT}^{j\nu}(x, \sigma, t, \mathbf{p}_{\perp}) &= \frac{1}{2} \int_0^{\xi_s} \frac{d\xi}{2\pi} e^{i\sigma \cdot \xi} \left[W_{[++]}^{\nu[i\sigma^{j+}\gamma^5]}(x, \xi, \Delta_{\perp}^2, \mathbf{p}_{\perp}^2, \mathbf{p}_{\perp} \cdot \Delta_{\perp}) + W_{[--]}^{\nu[i\sigma^{j+}\gamma^5]}(x, \xi, \Delta_{\perp}^2, \mathbf{p}_{\perp}^2, \mathbf{p}_{\perp} \cdot \Delta_{\perp}) \right] \\ &= \tilde{\rho}_{UT}^{j\nu}(x, \sigma, t, \mathbf{p}_{\perp}) - \frac{1}{M} \epsilon_{\perp}^{ij} p_{\perp}^i \tilde{\rho}_{BM}^{\nu}(x, \sigma, t, \mathbf{p}_{\perp}). \end{aligned} \quad (37)$$

The T-odd coefficients of transverse quark momentum \mathbf{p}_{\perp} terms of the above Wigner Distributions in longitudinal boost invariant space are separated as Sivers and Boer-Mulder and defined as

$$\tilde{\rho}_{Siv}^{\nu}(x, \sigma, t, \mathbf{p}_{\perp}) = - \int_0^{\xi_s} \frac{d\xi}{2\pi} e^{i\sigma \cdot \xi} \sqrt{1 - \xi^2} F_{1,2}^{o\nu}(x, \xi, t, \mathbf{p}_{\perp}^2, \Delta_{\perp} \cdot \mathbf{p}_{\perp}), \quad (38)$$

$$\tilde{\rho}_{BM}^{\nu}(x, \sigma, t, \mathbf{p}_{\perp}) = - \int_0^{\xi_s} \frac{d\xi}{2\pi} e^{i\sigma \cdot \xi} \frac{1}{\sqrt{1 - \xi^2}} H_{1,1}^{o\nu}(x, \xi, t, \mathbf{p}_{\perp}^2, \Delta_{\perp} \cdot \mathbf{p}_{\perp}), \quad (39)$$

These play crucial roll in the correlation between spin and transverse momentum that led to the Single spin asymmetries. The above definition of the Sivers and Boer-Mulder distribution provide pictures in boost invariant longitudinal position space of the T-odd sector which are useful for the experimental measurements. The real life experiments are restricted to non-zero skewness measurement of the distributions. The transverse energy transfer Δ_{\perp}^2 is replaced by the total momentum transfer t using the relation Eq.(14). In the above Eqs.(38, 39), the minus sign is included to maintain the consistency with the definition in TMD limit. The complete expression of the left-out part of the WDs $\tilde{\rho}_{TU}^{i\nu}(x, \sigma, t, \mathbf{p}_{\perp})$ and $\tilde{\rho}_{UT}^{j\nu}(x, \sigma, t, \mathbf{p}_{\perp})$ are included in App.A.

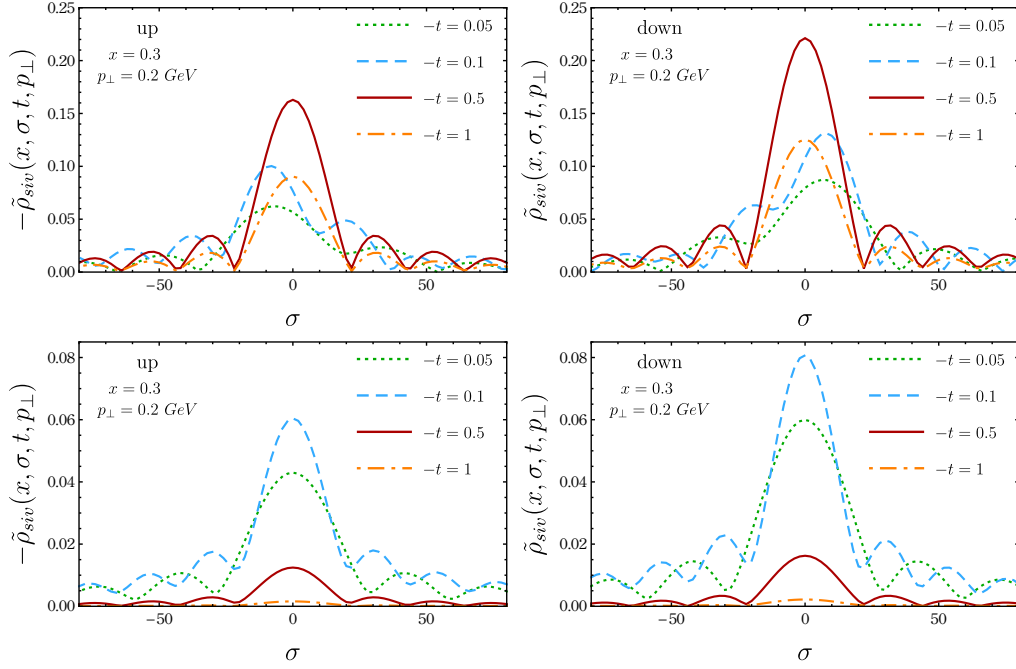


FIG. 5: Siverts Wigner distribution in boost invariant longitudinal space at $x = 0.3$, $\mathbf{p}_\perp = 0.2\hat{p}_y$ GeV along \hat{y} . The four plots in each sub-figures are for $-t = 0.05, 0.1, 0.5$, and 1 . The left and right column are for u -quark and d -quark respectively. The upper row shows the model results when \mathbf{p}_\perp and Δ_\perp are parallel, whereas the lower row is when \mathbf{p}_\perp and Δ_\perp are perpendicular i.e., $\mathbf{p}_\perp \cdot \Delta_\perp = 0$.

In Fig.5, the numerical plots of Siverts distribution $\tilde{\rho}_{Siv}^\nu(x, \sigma, t, \mathbf{p}_\perp)$ is shown in the boost invariant longitudinal at $x = 0.3$, $\mathbf{p}_\perp = 0.2\hat{p}_y$ GeV space for u (left) and d (right) quarks. Note that, the Siverts WDs in σ -space is negative for u quark and a minus sign is included in the axis label. In each of the plots, four different color-codes(line codes) are corresponding to the four fixed values of $-t = 0.05, 0.1, 0.5$ and 1 .

The distribution in boost invariant longitudinal space shows oscillating behaviour which is analogous to the optical diffraction phenomenon. The amplitude of the maxima of Siverts WDs in σ -space is larger for d -quark than the u -quark. Finiteness of the width of a slit is a necessary condition to achieve diffraction pattern in Optics. Here, the finite limit of the Fourier integration in ξ_s (from 0 to ξ_{max} or x) plays equivalent role to the slit width for occurrence of the diffraction pattern. For all the plots in σ -space, the width of principle maxima becomes narrower with the increase of ξ_{max} determined by larger energy transfer $-t$. This behaviour is similar to optical diffraction through slit where the position of the first minima varies inversely to the slit width.

For last two values of $-t = \{0.5, 1.0\}$, from Eq.(33) the corresponding $\xi_{max} = \{0.521, 0.639\}$ respectively, which belong to the region $\xi_{max} > x$ and the limit of the Fourier transform in Eq.(38) set to $\xi_s = x = 0.3$ for both the cases. As the upper limit of the Fourier transformation is fixed to $x = 0.3$, no changes are noticed in the position of first minima for $-t = \{0.5, 1.0\}$ marked by red continuous and orange dot-dashed lines. However the peak value of the central maxima changes significantly and the position of the central maxima reflects symmetric pattern for both the quarks.

For the first two choices of $-t = \{0.05, 0.1\}$, $\xi_{max} = \{0.211, 0.285\}$ respectively, which lie in the region $\xi_{max} < x$ (as $x = 0.3$) and the integration limit is set to $\xi_s = \xi_{max}$. Thus, the position of the first minima for $-t = 0.1$ is smaller than the position of the first minima for $-t = 0.05$. In other word, the width decreases as $-t$ increases in this region. Additionally, we have noticed that the pattern is no longer symmetric and show left shifting for u and right shifting for d quarks which are consistent with the left-right shift in quark density associated to Siverts effect as shown in Fig.4. We also have noticed a significant secondary maxima for both the quarks which is due to the dominating interference among \mathbf{p}_\perp and Δ_\perp in this region $\xi_{max} < x$. Here, the upper row of Fig.5 shows our model results when \mathbf{p}_\perp is chosen parallel to Δ_\perp . The terms contain $\mathbf{p}_\perp \cdot \Delta_\perp$ led to an asymmetric diffraction pattern which can be interpreted as an additional significant contribution from the interference over diffraction as found in Optics. For completeness, the Siverts distribution in σ -space is investigated vanishing the interference term by putting $\mathbf{p}_\perp \cdot \Delta_\perp = 0$ in Eq.(38) and shown in Fig.5(lower row). The $\mathbf{p}_\perp \cdot \Delta_\perp$ term generates from the square of transverse momentums of incoming \mathbf{p}'_\perp (Eq.20) and out going \mathbf{p}''_\perp (Eq.21) proton. Eventually, all the $(\chi_i - \chi_j)$ terms and the exponential factor contain

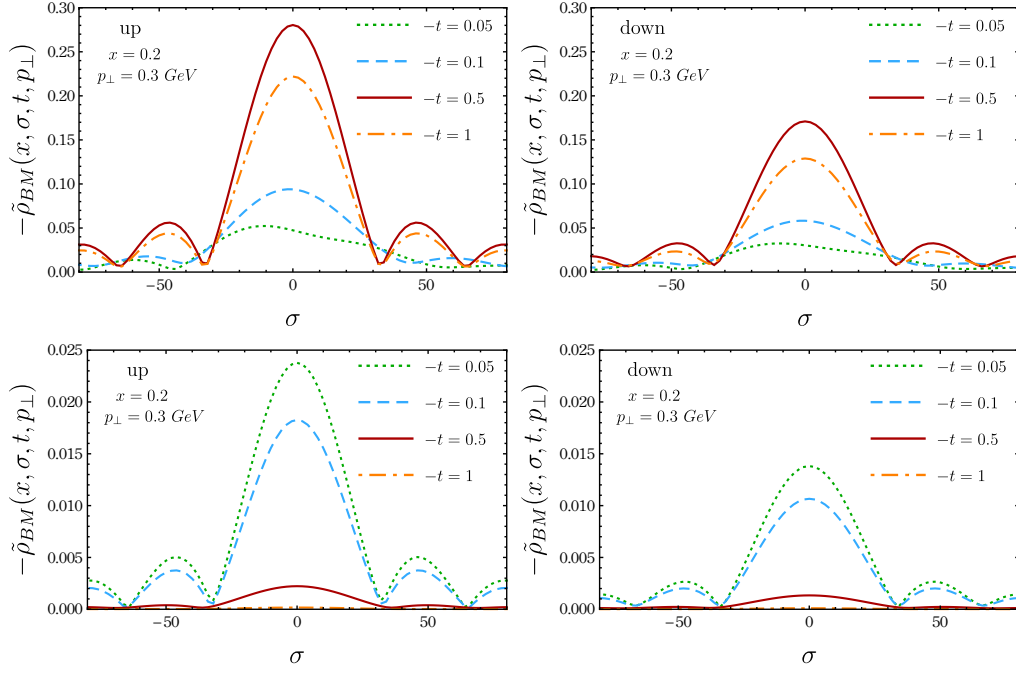


FIG. 6: Boer-Mulders Wigner distribution in boost invariant longitudinal space at $x = 0.3$, $\mathbf{p}_\perp = 0.2\hat{p}_y$ GeV along \hat{y} . The four plots in each sub-figures are for $-t = 0.05, 0.1, 0.5$, and 1 . The left and right column are for u -quark and d -quark respectively. The upper row shows the model results when \mathbf{p}_\perp and Δ_\perp are parallel, whereas the lower row is when \mathbf{p}_\perp and Δ_\perp are perpendicular i.e., $\mathbf{p}_\perp \cdot \Delta_\perp = 0$.

$\mathbf{p}_\perp \cdot \Delta_\perp$ term. We have noticed that, for the region $\xi_{max} < x$, the distribution becomes symmetric and the width of the central maxima decreases as the total momentum transfer $-t$ increases. The overall amplitude reduced by a large amount which reflects a significant amount of contribution is gettered from the $\mathbf{p}_\perp \cdot \Delta_\perp$ term in boost invariant longitudinal space. Thus, the diffraction pattern is not solely due to the finite limit of Fourier ξ integration, and the functional forms of the GTMDs are also important for this phenomenon.

This kind of oscillating behavior is not very exceptional, a similar paraxial optics and quantum fields on the light cone was first reported in [81, 82]. Notably, distributions in the boost invariant longitudinal space shows a long-distance tail as reported recently in Refs.[52, 83]. A qualitatively similar diffraction pattern has also been observed in other observables such as DVCS amplitude, GPDs, and the parton density in longitudinal position space [42–44, 48].

Fig.6, shows our model result of Boer-Mulder Wigner distribution in boost invariant longitudinal position space for u and d quarks. The similar diffraction pattern is noticed caused by the finite integration limit in Fourier transformation in Eq(39). The model result for Boer-Mulders Wigner distribution is negative for both the quarks, while the peak of maxima are larger for u quark than the d quark. The change in polarity from u to d quark justifies the left-right symmetry for the Siverts function, whereas Boer-Mulders distribution does not show any change in polarity which led to one directional shift in spin density. This difference can be justified from the model results of $F_{1,2}$ and $H_{1,1}$ GTMDs shown in Fig.2. The upper row is the model result when \mathbf{p}_\perp is parallel to Δ_\perp and a less significant interference is noticed for the region $\xi_{max} < x$ compare to Siverts distribution. This can be understood from the model result of $H_{1,1}$ which does not have the third term (Eq.24) containing $(\chi_2'' - \chi_2')$ term like Siverts distribution. The lower row of Fig.6 represents the model results when \mathbf{p}_\perp and Δ_\perp are perpendicular to each other and the distribution becomes symmetric as expected.

V. SIVERS AND BOER-MULDERS DISTRIBUTION IN \mathbf{b}_\perp -SPACE

For completeness, in this section we present the Siverts and Boer-Mulders WDs in transverse impact parameter space denoted by \mathbf{b}_\perp . The impact parameter \mathbf{b}_\perp is conjugate to $\mathbf{D}_\perp = \Delta_\perp / (1 - \xi^2)$ and using this relation the Δ_\perp

is replaced by \mathbf{D}_\perp . The real part of the modified Wigner distribution $\bar{\rho}_{TU}^{\nu\nu}(x, \xi, \mathbf{b}_\perp, \mathbf{p}_\perp)$ is given by

$$\begin{aligned}\bar{\rho}_{TU}^{\nu\nu}(x, \xi, \mathbf{b}_\perp, \mathbf{p}_\perp) &= -\frac{1}{2} \int \frac{d^2 \mathbf{D}_\perp}{(2\pi)^2} e^{-i\mathbf{D}_\perp \cdot \mathbf{b}_\perp} \epsilon_\perp^{ij} (i)^j \left[W_{[+-]}^{\nu[\gamma^+]}(x, \xi, \mathbf{D}_\perp, \mathbf{p}_\perp) + (-1)^j W_{[-+]}^{\nu[\gamma^+]}(x, \xi, \mathbf{D}_\perp, \mathbf{p}_\perp) \right] \\ &= \rho_{TU}^{\nu\nu}(x, \xi, \mathbf{b}_\perp, \mathbf{p}_\perp) + \frac{1}{M} \epsilon_\perp^{ij} p_\perp^j \bar{\rho}_{Siv}^\nu(x, \xi, \mathbf{b}_\perp, \mathbf{p}_\perp),\end{aligned}\quad (40)$$

$$\begin{aligned}\bar{\rho}_{UT}^{\nu\nu}(x, \xi, \mathbf{b}_\perp, \mathbf{p}_\perp) &= \frac{1}{2} \int \frac{d^2 \mathbf{D}_\perp}{(2\pi)^2} e^{-i\mathbf{D}_\perp \cdot \mathbf{b}_\perp} \left[W_{[++]}^{\nu[i\sigma^{j+}\gamma^5]}(x, \xi, \mathbf{D}_\perp, \mathbf{p}_\perp) + W_{[--]}^{\nu[i\sigma^{j+}\gamma^5]}(x, \xi, \mathbf{D}_\perp, \mathbf{p}_\perp) \right] \\ &= \rho_{UT}^{\nu\nu}(x, \xi, \mathbf{b}_\perp, \mathbf{p}_\perp) - \frac{1}{M} \epsilon_\perp^{ij} p_\perp^i \bar{\rho}_{BM}^\nu(x, \xi, \mathbf{b}_\perp, \mathbf{p}_\perp).\end{aligned}\quad (41)$$

Where, $\rho_{TU}^{\nu\nu}(x, \xi, \mathbf{b}_\perp, \mathbf{p}_\perp)$ and $\rho_{UT}^{\nu\nu}(x, \xi, \mathbf{b}_\perp, \mathbf{p}_\perp)$ are the T-even part without the FSI contribution and included the explicit forms in Appendix-A. We define the Fourier transform of the T-odd GTMDs $F_{1,2}^o$ and $H_{1,1}^o$ as Siverson and Boer-Mulders Wigner distribution respectively as

$$\bar{\rho}_{Siv}^\nu(x, \xi, \mathbf{b}_\perp, \mathbf{p}_\perp) = - \int \frac{d^2 \mathbf{D}_\perp}{(2\pi)^2} e^{-i\mathbf{D}_\perp \cdot \mathbf{b}_\perp} \sqrt{1 - \xi^2} F_{1,2}^{o\nu}(x, \xi, \mathbf{D}_\perp, \mathbf{p}_\perp), \quad (42)$$

$$\bar{\rho}_{BM}^\nu(x, \xi, \mathbf{b}_\perp, \mathbf{p}_\perp) = - \int \frac{d^2 \mathbf{D}_\perp}{(2\pi)^2} e^{-i\mathbf{D}_\perp \cdot \mathbf{b}_\perp} \frac{1}{\sqrt{1 - \xi^2}} H_{1,1}^{o\nu}(x, \xi, \mathbf{D}_\perp, \mathbf{p}_\perp), \quad (43)$$

These are the most general form of the Siverson and Boer-Mulders function having the dependency on the kinematics $(x, \xi, \mathbf{b}_\perp, \mathbf{p}_\perp)$.

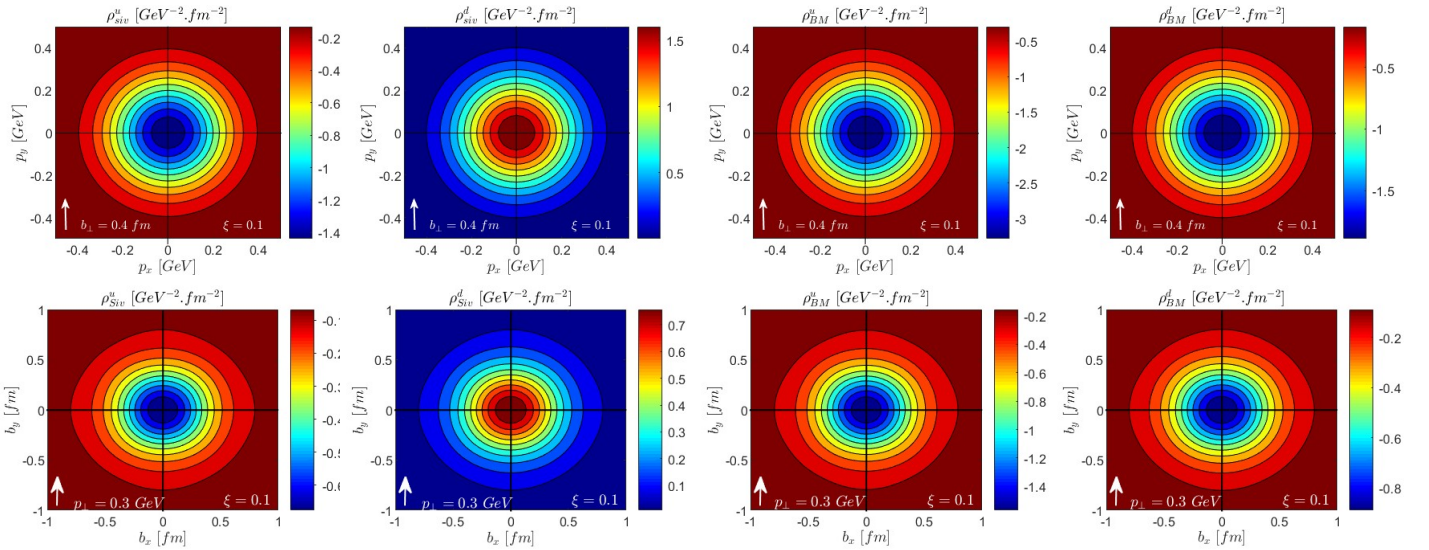


FIG. 7: The flavor dependent Siverson and Boer-Mulders Wigner Distribution in transverse momentum plane (upper row) with $\mathbf{b}_\perp = 0.4 \hat{y}$ and transverse impact parameter plane (lower row) with $\mathbf{p}_\perp = 0.3 \text{ GeV}$ at skewness $\xi = 0.1$.

We investigate these functions numerically in the transverse momentum and transverse position space. The model results for Siverson function as a function of transverse impact parameter space are shown in Fig.7. The upper row represents momentum space distribution with non-zero skewness $\xi = 0.1$ at $\mathbf{b}_\perp = 0.4 \text{ fm}$ along \hat{y} for both the flavors. While the lower row is for transverse impact parameter plane with skewness $\xi = 0.1$ at $\mathbf{p}_\perp = 0.3 \text{ GeV}$ along \hat{y} . We notice polarity flip with the change in flavor in both the \mathbf{p}_\perp and \mathbf{b}_\perp planes which are at per our expectation of model results of positive and negative $F_{1,2}^o$ distributions under flavor change. For numerical calculation, we choose the transverse momentum transfer $\mathbf{\Delta}_\perp$ is parallel to the transverse momentum to the quark \mathbf{p}_\perp . The circularly symmetric contour plots in \mathbf{p}_\perp -plane indicates insignificant contribution from the crossing terms containing $\mathbf{p}_\perp \cdot \mathbf{\Delta}_\perp$. While, transverse impact parameter plane \mathbf{b}_\perp -plane distribution is no longer circularly symmetric caused by the terms contain $\mathbf{p}_\perp \cdot \mathbf{\Delta}_\perp$ and shows an axial-symmetry. We also noticed that, for both the plane, intensity of the Siverson WDs decreases for increasing skewness ξ . The model results for Boer-Mulders distribution shows similar pasterns- \mathbf{p}_\perp -plane is circularly symmetric where as \mathbf{b}_\perp -plane is axially symmetric, as shown in Fig.7. Note that, Siverson distributions is part of the Wigner distribution for unpolarised quark in a transversely polarised proton $\bar{\rho}_{TU}^{\nu\nu}(x, \xi, \mathbf{b}_\perp, \mathbf{p}_\perp)$, which shows

an dipole structure in \mathbf{b}_\perp -plane caused by the transverse momentum cross-terms present in first part of Eq.40. The axially symmetric Sivers distribution is considered as an enhancement in intensity preserving the di-polar structure in \mathbf{b}_\perp -plane. The intensity of the distributions are sensitive to the skewness given by this model may useful for phenomenological study of experimental measurements.

VI. CONCLUSIONS

In continuation to our previous work on GTMDs and WDs with skewness, that focused on T-even sector of GTMDs and Wigner Distributions [46], here we concentrate on the skewness sensitivity of the T-odd sector considering the momentum transfer in both the transverse and the longitudinal directions. Our work is thus well-suited for proper analysis of experimental data which are measured considering non-zero skewness. We present a generalised form of the Sivers and Boer-Mulders distribution encoding information of momentum and impact parameters space. The primary focus of this work is a detailed model study on Sivers and Boer-Mulders WDs in boost invariant longitudinal position space σ which is conjugate to the skewness ξ .

The leading twist T-odd GTMDs in proton are investigated using light-front quark-diquark model motivated by soft-wall AdS/QCD. In both ξ - x plane and x - Δ_\perp plane, the model results for GTMDs $F_{1,2}^o$ show a sign flip under change in flavor while and polarity of $H_{1,1}^o$ remain same irrespective of flavor. That leads to the study of ξ sensitivity of spin transverse momentum correlation. All the numerical results are shown in the DGLAP region, i.e., for $\xi < x < 1$. The magnitude of both $F_{1,2}^o$ and $H_{1,1}^o$ die out with the increase of ξ and peak shift towards right upto $x < 0.5$. The Fourier transformation of skewness dependent T-odd GTMDs lead to boost invariant longitudinal position space configuration of Sivers and Boer-Mulders Wigner distributions. The LQDM model results of Sivers and Boer-Mulders distribution, over a finite limit Fourier transformation given by square of the energy transfer $-t$, show an oscillatory behaviour analogous to diffraction phenomenon in wave optics. The width of the central diffraction maxima is sensitive to the square of momentum transfer $-t$. As $-t$ increases, the width of principal maxima becomes narrower. Such inverse variation in diffraction resembles relation between slit width and wavelength in wave optics and here, the square of momentum transfer $-t$ plays a similar role to effective slit-width. However, such diffraction pattern is not solely due to finiteness of Fourier limit over ξ but the functional behaviours of the GTMDs are crucial. In this model the correlation among \mathbf{p}_\perp and Δ_\perp plays an crucial role— if \mathbf{p}_\perp is perpendicular to Δ_\perp , the diffraction pattern is symmetric like a single-slit diffraction pattern, while if both are parallel to each other, the diffraction pattern lost its symmetry. Which can be thought of an effect caused by interference between \mathbf{p}_\perp and Δ_\perp . Such interference effects demands other model calculation or future experimental measurement for verification. A similar diffraction pattern has also been observed in several other observable such as DVCS amplitude, GPDs, and the parton density in longitudinal position space.

For completeness, the Sivers and Boer-Mulders WDs are also presented in transverse momentum space as well as in transverse impact parameter space. The model result shows a circular symmetry in \mathbf{p}_\perp -plane where as axial symmetry in \mathbf{b}_\perp -plane which is consider as an additional contribution form T-odd sector to the complete Wigner Distribution of unpolarised quark in a transversely polarised proton.

Acknowledgments

The work of T. M. is supported by the Science and Engineering Research Board (SERB) through the SRG (Start-up Research Grant) of File No. SRG/2023/001093.

Appendix A

The spinors $u(k, \lambda)$ with the momentum k and the helicity $\lambda (= \pm)$ are given by

$$u(k, +) = \frac{1}{\sqrt{2k^+}} \begin{pmatrix} k^+ + m_F \\ k^1 + ik^2 \\ k^+ - m_F \\ k^1 + ik^2 \end{pmatrix}, \quad u(k, -) = \frac{1}{\sqrt{2k^+}} \begin{pmatrix} -k^1 + ik^2 \\ k^+ + m_F \\ k^1 - ik^2 \\ -k^+ + m_F \end{pmatrix}$$

with m_F being the mass of the fermion. Using the kinematics given in Eqs. (11), (12), one can find out the spinors $u(P', \lambda')$ and $u(P'', \lambda'')$ and compute the matrix elements of $\bar{u}(k, \lambda)\Gamma u(k, \lambda)$, where Γ represents the Dirac matrix structure.

The explicit expression of $\hat{\rho}_{UT}^{j\nu}(x, \sigma, t, \mathbf{p}_\perp)$ and $\hat{\rho}_{TU}^{j\nu}(x, \sigma, t, \mathbf{p}_\perp)$ in Eq.(36) and Eq.(37) can be expressed in terms of GTMDs as

$$\hat{\rho}_{TU}^{j\nu}(x, \sigma, t, \mathbf{p}_\perp) = \int_0^{\xi_s} \frac{d\xi}{2\pi} e^{i\sigma\xi} \frac{-i}{2M\sqrt{1-\xi^2}} \epsilon_\perp^{ij} \left[\Delta_\perp^j \left(F_{1,1}^\nu(x, \xi, t, \mathbf{p}_\perp^2, \Delta_\perp \cdot \mathbf{p}_\perp) - 2(1-\xi^2) F_{1,3}^\nu(x, \xi, t, \mathbf{p}_\perp^2, \Delta_\perp \cdot \mathbf{p}_\perp) \right) \right. \\ \left. - 2(1-\xi^2) p_\perp^j F_{1,2}^{(e)\nu}(x, \xi, t, \mathbf{p}_\perp^2, \Delta_\perp \cdot \mathbf{p}_\perp) + \frac{\xi}{M^2} \epsilon_\perp^{kl} p_\perp^k \Delta_\perp^l \Delta_\perp^j F_{1,4}^{(e)\nu}(x, \xi, t, \mathbf{p}_\perp^2, \Delta_\perp \cdot \mathbf{p}_\perp) \right], \quad (\text{A1})$$

$$\hat{\rho}_{UT}^{j\nu}(x, \sigma, t, \mathbf{p}_\perp) = \int_0^{\xi_s} \frac{d\xi}{2\pi} e^{i\sigma\xi} \frac{-i}{M\sqrt{1-\xi^2}} \epsilon_\perp^{ij} \left[p_\perp^i H_{1,1}^{(e)\nu}(x, \xi, t, \mathbf{p}_\perp^2, \Delta_\perp \cdot \mathbf{p}_\perp) + \Delta_\perp^i H_{1,2}^\nu(x, \xi, t, \mathbf{p}_\perp^2, \Delta_\perp \cdot \mathbf{p}_\perp) \right], \quad (\text{A2})$$

Note that, the first term of Eq.(40) and in Eq.(41) have similar decomposition in terms of GTMDs for the Fourier transform in the \mathbf{b}_\perp space.

-
- [1] P. J. Mulders and R. D. Tangerman, Nucl. Phys. B **461**, 197 (1996), [Erratum: Nucl.Phys.B 484, 538–540 (1997)], hep-ph/9510301.
 - [2] V. Barone, A. Drago, and P. G. Ratcliffe, Phys. Rept. **359**, 1 (2002), hep-ph/0104283.
 - [3] A. Bacchetta, M. Diehl, K. Goeke, A. Metz, P. J. Mulders, and M. Schlegel, JHEP **02**, 093 (2007), hep-ph/0611265.
 - [4] S. J. Brodsky, D. S. Hwang, and I. Schmidt, Phys. Lett. B **530**, 99 (2002), hep-ph/0201296.
 - [5] A. Bacchetta, F. Delcarro, C. Pisano, M. Radici, and A. Signori, JHEP **06**, 081 (2017), [Erratum: JHEP 06, 051 (2019)], 1703.10157.
 - [6] X.-D. Ji, Phys. Rev. D **55**, 7114 (1997), hep-ph/9609381.
 - [7] M. Diehl, Phys. Rept. **388**, 41 (2003), hep-ph/0307382.
 - [8] A. V. Belitsky and A. V. Radyushkin, Phys. Rept. **418**, 1 (2005), hep-ph/0504030.
 - [9] K. Goeke, M. V. Polyakov, and M. Vanderhaeghen, Prog. Part. Nucl. Phys. **47**, 401 (2001), hep-ph/0106012.
 - [10] D. W. Sivers, Phys. Rev. D **41**, 83 (1990).
 - [11] D. Boer and P. J. Mulders, Phys. Rev. D **57**, 5780 (1998), hep-ph/9711485.
 - [12] S. Bhattacharya, A. Metz, and J. Zhou, Phys. Lett. B **771**, 396 (2017), [Erratum: Phys.Lett.B 810, 135866 (2020)], 1702.04387.
 - [13] Y. Hatta, B.-W. Xiao, and F. Yuan, Phys. Rev. Lett. **116**, 202301 (2016), 1601.01585.
 - [14] X. Ji, F. Yuan, and Y. Zhao, Phys. Rev. Lett. **118**, 192004 (2017), 1612.02438.
 - [15] Y. Hatta, Y. Nakagawa, F. Yuan, Y. Zhao, and B. Xiao, Phys. Rev. D **95**, 114032 (2017), 1612.02445.
 - [16] S. Bhattacharya, R. Boussarie, and Y. Hatta (2022), 2201.08709.
 - [17] Y. Hagiwara, Y. Hatta, R. Pasechnik, M. Tasevsky, and O. Teryaev, Phys. Rev. D **96**, 034009 (2017), 1706.01765.
 - [18] J. Zhou, Phys. Rev. D **94**, 114017 (2016), 1611.02397.
 - [19] M. Diehl, Eur. Phys. J. C **25**, 223 (2002), [Erratum: Eur.Phys.J.C 31, 277–278 (2003)], hep-ph/0205208.
 - [20] M. Burkardt, Int. J. Mod. Phys. A **18**, 173 (2003), hep-ph/0207047.
 - [21] J. P. Ralston and B. Pire, Phys. Rev. D **66**, 111501 (2002), hep-ph/0110075.
 - [22] N. Kaur, N. Kumar, C. Mondal, and H. Dahiya, Nucl. Phys. B **934**, 80 (2018), 1807.01076.
 - [23] D. Chakrabarti, T. Maji, C. Mondal, and A. Mukherjee, Phys. Rev. D **95**, 074028 (2017), 1701.08551.
 - [24] X.-d. Ji, Phys. Rev. Lett. **91**, 062001 (2003), hep-ph/0304037.
 - [25] C. Lorce, B. Pasquini, X. Xiong, and F. Yuan, Phys. Rev. D **85**, 114006 (2012), 1111.4827.
 - [26] C. Lorce and B. Pasquini, Phys. Rev. D **84**, 014015 (2011), 1106.0139.
 - [27] C. Lorce, B. Pasquini, and M. Vanderhaeghen, JHEP **05**, 041 (2011), 1102.4704.
 - [28] A. Mukherjee, S. Nair, and V. K. Ojha, Phys. Rev. D **90**, 014024 (2014), 1403.6233.
 - [29] A. Mukherjee, S. Nair, and V. K. Ojha, Phys. Rev. D **91**, 054018 (2015), 1501.03728.
 - [30] J. More, A. Mukherjee, and S. Nair, Phys. Rev. D **95**, 074039 (2017), 1701.00339.
 - [31] T. Liu and B.-Q. Ma, Phys. Rev. D **91**, 034019 (2015), 1501.07690.
 - [32] D. Chakrabarti, T. Maji, C. Mondal, and A. Mukherjee, Eur. Phys. J. C **76**, 409 (2016), 1601.03217.
 - [33] D. Chakrabarti, N. Kumar, T. Maji, and A. Mukherjee, Eur. Phys. J. Plus **135**, 496 (2020), 1902.07051.
 - [34] T. Gutsche, V. E. Lyubovitskij, and I. Schmidt, Eur. Phys. J. C **77**, 86 (2017), 1610.03526.
 - [35] S. Kaur and H. Dahiya, Adv. High Energy Phys. **2020**, 9429631 (2020), 1906.04662.
 - [36] N. Kumar and C. Mondal, Nucl. Phys. B **931**, 226 (2018), 1705.03183.
 - [37] K. Kanazawa, C. Lorcé, A. Metz, B. Pasquini, and M. Schlegel, Phys. Rev. D **90**, 014028 (2014), 1403.5226.
 - [38] Z.-L. Ma and Z. Lu, Phys. Rev. D **98**, 054024 (2018), 1808.00140.
 - [39] S. Kaur and H. Dahiya, Phys. Rev. D **100**, 074008 (2019), 1908.01939.
 - [40] N. Kaur and H. Dahiya, Eur. Phys. J. A **56**, 172 (2020), 1909.10146.
 - [41] J.-L. Zhang and J.-L. Ping, Eur. Phys. J. C **81**, 814 (2021).
 - [42] S. J. Brodsky, D. Chakrabarti, A. Harindranath, A. Mukherjee, and J. P. Vary, Phys. Rev. D **75**, 014003 (2007), hep-ph/0611159.

- [43] D. Chakrabarti, R. Manohar, and A. Mukherjee, Phys. Rev. D **79**, 034006 (2009), 0811.0521.
- [44] R. Manohar, A. Mukherjee, and D. Chakrabarti, Phys. Rev. D **83**, 014004 (2011), 1012.2627.
- [45] N. Kumar and H. Dahiya, Int. J. Mod. Phys. A **30**, 1550010 (2015), 1501.04745.
- [46] T. Maji, C. Mondal, and D. Kang, Phys. Rev. D **105**, 074024 (2022), 2202.08635.
- [47] V. K. Ojha, S. Jana, and T. Maji, Phys. Rev. D **107**, 074040 (2023), 2211.02959.
- [48] S. J. Brodsky, D. Chakrabarti, A. Harindranath, A. Mukherjee, and J. P. Vary, Phys. Lett. B **641**, 440 (2006), hep-ph/0604262.
- [49] C. Mondal and D. Chakrabarti, Eur. Phys. J. C **75**, 261 (2015), 1501.05489.
- [50] C. Mondal, Eur. Phys. J. C **77**, 640 (2017), 1709.06877.
- [51] D. Chakrabarti and C. Mondal, Phys. Rev. D **92**, 074012 (2015), 1509.00598.
- [52] G. A. Miller and S. J. Brodsky, Phys. Rev. C **102**, 022201 (2020), 1912.08911.
- [53] T. Maji and D. Chakrabarti, Phys. Rev. D **94**, 094020 (2016), 1608.07776.
- [54] T. Maji, C. Mondal, D. Chakrabarti, and O. V. Teryaev, JHEP **01**, 165 (2016), 1506.04560.
- [55] T. Maji and D. Chakrabarti, Phys. Rev. D **95**, 074009 (2017), 1702.04557.
- [56] T. Maji, C. Mondal, and D. Chakrabarti, Phys. Rev. D **96**, 013006 (2017), 1702.02493.
- [57] T. Maji, D. Chakrabarti, and O. V. Teryaev, Phys. Rev. D **96**, 114023 (2017), 1711.01746.
- [58] T. Maji, D. Chakrabarti, and A. Mukherjee, Phys. Rev. D **97**, 014016 (2018), 1711.02930.
- [59] N. Kumar, C. Mondal, and N. Sharma, Eur. Phys. J. A **53**, 237 (2017), 1712.02110.
- [60] R. Jakob, P. J. Mulders, and J. Rodrigues, Nucl. Phys. A **626**, 937 (1997), hep-ph/9704335.
- [61] A. Bacchetta, F. Conti, and M. Radici, Phys. Rev. D **78**, 074010 (2008), 0807.0323.
- [62] G. P. Lepage and S. J. Brodsky, Phys. Rev. D **22**, 2157 (1980).
- [63] J. R. Ellis, D. S. Hwang, and A. Kotzinian, Phys. Rev. D **80**, 074033 (2009), 0808.1567.
- [64] S. J. Brodsky and G. F. de Teramond, Phys. Rev. D **77**, 056007 (2008), 0707.3859.
- [65] G. F. de Teramond and S. J. Brodsky, in *Ferrara International School Niccolò Cabeo 2011: Hadronic Physics* (2011), pp. 54–109, 1203.4025.
- [66] D. Chakrabarti and C. Mondal, Eur. Phys. J. C **73**, 2671 (2013), 1307.7995.
- [67] D. Chakrabarti and C. Mondal, Phys. Rev. D **88**, 073006 (2013), 1307.5128.
- [68] S. Meissner, A. Metz, M. Schlegel, and K. Goeke, JHEP **08**, 038 (2008), 0805.3165.
- [69] S. Meissner, A. Metz, and M. Schlegel, JHEP **08**, 056 (2009), 0906.5323.
- [70] S. J. Brodsky, M. Diehl, and D. S. Hwang, Nucl. Phys. B **596**, 99 (2001), hep-ph/0009254.
- [71] D. Chakrabarti, P. Choudhary, B. Gurjar, T. Maji, C. Mondal, and A. Mukherjee, Phys. Rev. D **109**, 114040 (2024), 2402.16503.
- [72] X.-D. Ji, W. Melnitchouk, and X. Song, Phys. Rev. D **56**, 5511 (1997), hep-ph/9702379.
- [73] S. Scopetta and V. Vento, Eur. Phys. J. A **16**, 527 (2003), hep-ph/0201265.
- [74] V. Y. Petrov, P. V. Pobylitsa, M. V. Polyakov, I. Bornig, K. Goeke, and C. Weiss, Phys. Rev. D **57**, 4325 (1998), hep-ph/9710270.
- [75] M. Penttinen, M. V. Polyakov, and K. Goeke, Phys. Rev. D **62**, 014024 (2000), hep-ph/9909489.
- [76] S. Boffi, B. Pasquini, and M. Traini, Nucl. Phys. B **649**, 243 (2003), hep-ph/0207340.
- [77] A. Vega, I. Schmidt, T. Gutsche, and V. E. Lyubovitskij, Phys. Rev. D **83**, 036001 (2011), 1010.2815.
- [78] G. F. de Teramond, T. Liu, R. S. Sufian, H. G. Dosch, S. J. Brodsky, and A. Deur (HLFHS), Phys. Rev. Lett. **120**, 182001 (2018), 1801.09154.
- [79] S. Xu, C. Mondal, J. Lan, X. Zhao, Y. Li, and J. P. Vary (BLFQ), Phys. Rev. D **104**, 094036 (2021), 2108.03909.
- [80] A. Bacchetta, U. D'Alesio, M. Diehl, and C. A. Miller, Phys. Rev. D **70**, 117504 (2004), hep-ph/0410050.
- [81] E. C. G. Sudarshan, R. Simon, and N. Mukunda, Phys. Rev. A **28**, 2921 (1983).
- [82] N. Mukunda, R. Simon, and E. C. G. Sudarshan, Phys. Rev. A **28**, 2933 (1983).
- [83] C. M. Weller and G. A. Miller (2021), 2111.03194.